Journal of Applied Polymer Science

Simultaneous Enhancements in the Mechanical, Thermal, and Electrical Performances of Glass-Fiber-Reinforced Cyanate Ester/Epoxy Composites with Plasma-Functionalized Carbon Nanotubes at Different Temperatures

Jingwen Li,[1,2] Zhixiong Wu,[1] Chuanjun Huang,[1] Youping Tu,[3] Laifeng Li[1]

[1]Key Laboratory of Cryogenics, Technical Institute of Physics and Chemistry, Chinese Academy of Sciences, Beijing 100190, PR China

[2]University of Chinese Academy of Sciences, Beijing 100049, PR China

[3]North China Electric Power University, Beijing 102206, PR China

Correspondence to: L. Li (E-mail: laifengli@mail.ipc.ac.cn) and Z. Wu (E-mail: zxwu@mail.ipc.ac.cn)

ABSTRACT: Woven glass-fiber-reinforced cyanate ester/epoxy composites modified with plasma-functionalized multiwalled carbon nanotubes (MWCNTs) were prepared. The mechanical, thermal, and electrical properties of the composites were investigated at different temperatures. The results show that the interlaminar shear strength, thermal conductivity, and electrical conductivity of the composites at room temperature and the cryogenic temperatures were enhanced simultaneously by the incorporation of MWCNTs, whereas the nonconductive behavior of the composites as electrical insulating materials was not changed. Meanwhile, the reinforcing mechanism was also examined on the basis of the microstructure of the composites. © 2014 Wiley Periodicals, Inc. J. Appl. Polym. Sci. **2015**, *132*, 41418.

KEYWORDS: composites; fibers; graphene and fullerenes; nanotubes; properties and characterization; resins

Received 24 June 2014; accepted 14 August 2014
DOI: 10.1002/app.41418

INTRODUCTION

Glass-fiber-reinforced polymer (GFRP) composites are widely used in many areas, including aerospace, superconducting magnets, and electrical packaging.[1,2] The glass-fiber-woven-reinforced cyanate ester/epoxy systems attract much attention for their excellent performance, which includes good mechanical properties, good radiation resistance,[3] low moisture absorption,[4] and long pot life of the matrix;[5] this combines the advantages of two types of high-performance thermosetting resins. However, with the development of many industries, such as cryogenic engineering, charge-storage capacitors, and electrical packaging, better properties, in terms of the mechanical strength, thermal conductivity, and electrical resistance, are required. For example, a relatively high electrical conductivity is required to provide electrostatic discharge for the insulating the polymer matrix in aircraft applications.[6] Especially, when the temperature decreases to cryogenic temperatures, the polymer matrix becomes brittle, and the thermal conductivity becomes much lower than that at room temperature (RT). However, the high cryogenic mechanical strength and relatively high thermal conductivity of GFRP composites are required for some equipment operating at cryogenic temperatures, such as aerospace engineering and superconducting magnets.[7]

The addition of corresponding fillers may be an effective way to modify GFRP composites to meet these requirements. The properties of the composites are changed by the addition of corresponding fillers, including ceramics, carbon fibers, and carbon nanotubes (CNTs). Lin et al.[8] introduced a small amount of organoclays to glass-fiber/epoxy composites and found that the flexural modulus and thermal stability values of the composites were enhanced. Wooster et al.[9] added silica into the cyanate ester matrix and enhanced the thermal conductivity and Young's modulus and decreased the thermal expansion.

CNTs have been considered candidate fillers for enhancing the properties of GFRP composites, because of their intrinsic outstanding mechanical properties (high aspect ratio, high Young's modulus, and tensile strength) and thermal and electrical conductivity. Gojny et al.[10] found that the interlaminar shear strength (ILSS) increased by 20% compared with the matrix-dominated ILSS with the addition of 0.3 wt % double-wall carbon nanotubes (DWCNTs) into GFRP composite, and the electrical conductivity of the system was also enhanced. Shen et al.[11] showed that the flexural strength and the thermal conductivity of the GFRP laminates were improved by 36 and 42%, respectively, with the addition of 2 wt % multiwalled carbon

nanotubes (MWCNTs). These studies have mainly focused on the enhanced properties at RT. However, when the temperature decreases to cryogenic temperatures, the matrix becomes brittle, and the thermal conductivity becomes lower than at RT. Few studies have examined the cryogenic properties of GFRP modified with MWCNTs. In this study, we focused on the improved properties of GFRP at both RT and cryogenic temperature with the addition of MWCNTs.

In addition, two main problems in terms of the dispersion and interfacial bonding have to be solved to ensure the efficient transference of the mechanical, thermal, and electrical properties from CNTs to polymer. Because of large van der Waal's forces, CNTs tend to aggregate; this leads to poor dispersion in the polymer matrix. Another problem is the weak interfacial bonding between the CNTs and the polymer matrix, which are due to the smooth surface of the CNTs.[12] To solve these two problem, a novel and effective method to functionalize the MWCNT surface was developed in our previous work.[13] An ultrathin poly(acrylic acid) (PAA) film was deposited on the MWCNT surface with a plasma polymerization approach. The dispersion of MWCNTs in the cyanate ester/epoxy matrix and the interfacial bonding strength between the MWCNTs and the matrix were significantly enhanced. Meanwhile, we also studied the mechanical properties of the MWCNT composites at RT and cryogenic temperature. The plasma-functionalized MWCNT composites showed much greater improvement than the as-received MWCNT composites.[14]

In our research, a small amount of PAA-functionalized MWCNTs were introduced into glass-fiber-woven-reinforced cyanate ester/epoxy resin systems. The composites were prepared with vacuum pressure impregnation (VPI). Meanwhile, a systematic study of the mechanical, thermal, and electrical properties at different temperatures was carried out. The ILSS of the composites was investigated at both RT and cryogenic temperature. The thermal conductivity and electrical properties as function of the temperature, which ranged from 77 K to RT, were also investigated.

EXPERIMENTAL

Materials

The epoxy resin and cyanate ester used in this study were diglycidyl ether of bisphenol F (GY285 from Huntsman), and 1,1-bis(4-cyanatophenyl)ethane (Primaset LECy from Lonza), respectively. The catalyst, acetylacetone cobalt(II), was provided by Alfa Aesar. The MWCNTs were provided by Chengdu Organic Chemicals Co., Ltd., and had dimensions of 30–50 nm in external diameter, 5–10 nm in internal diameter, and 10–20 μm in length. The glass-fiber fabric was a boron-free, 240 g/m^2 plain weave with 18 threads/cm in the warp (length), 14 threads/cm in the fill (width), treated by a silane agent (RW220-90 from Sinoma Science and Technology Co., Ltd., China). Acrylic acid, used as a monomer for plasma deposition because of its high saturation vapor pressure, was purchased from Beijing Yili Fine Chemical Co., Ltd.

Manufacturing

The manufacturing process of the MWCNT-reinforced glass-fiber/cyanate ester/epoxy composites consisted of two stages: (1) the preparation of MWCNT/cyanate ester/epoxy suspensions and (2) the preparation of the composites.

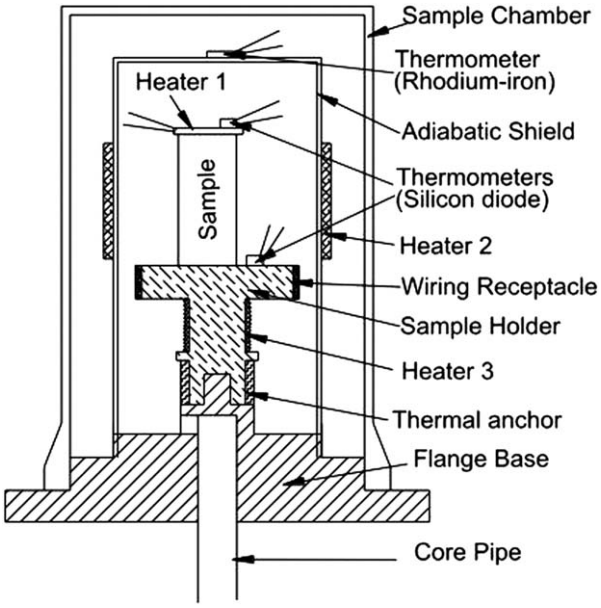

Figure 1. Schematic of the homemade equipment for the thermal conductivity measurements.

Preparation of the MWCNT/Cyanate Ester/Epoxy Mixtures. The mixture was prepared by the following procedure. First, the PAA-functionalized MWCNTs were prepared by a plasma polymerization process as reported in our previous study, and the thickness of the grafted PAA layer was about 3 nm.[13] Then, the blends containing 60 wt % cyanate ester and 40 wt % epoxy resin with 0.1 wt % catalyst were premixed in a 250-mL beaker. After that, the MWCNTs were dispersed into the blends with a tip sonicator for 30 min at a power of 230 W. The mixture was magnetically stirred and degassed with a vacuum pump at 45°C for about 3 h until the mixture was free of air bubbles.

Preparation of the Composites. The impregnation method explored in this study was VPI. GFRP composites with MWCNT contents of 0, 0.1, 0.3, and 0.5 wt % were prepared, and the thickness of the specimens were 4 and 0.5 mm. Before the impregnation, 6 × 18 cm^2 woven glass-fiber pieces were cut and sealed into a metal mold, which was coated with releasing agent. The metal mold together with woven glass fiber was dried at 100°C for 10 h. The bubble-freed mixtures were impregnated into the preheated mold and were cured at 150°C for 3 h and then 180°C for 3 h.

Characterization

Viscosity Measurements. The viscosity of the mixtures was measured by a Brookfield DV 2 Pro viscometer equipped with a small sample container (6.7 mL) at 45°C. The temperature was controlled by a recirculating thermal fluid around the sample container.

Short-Beam Shear (SBS) Tests. ILSS was determined by SBS test according to ASTM D 2344. The SBS tests were carried out on a SUNS 5000 test machine at 77 and 300 K with a crosshead speed of 1.5 mm/min. The test at 77 K was performed by

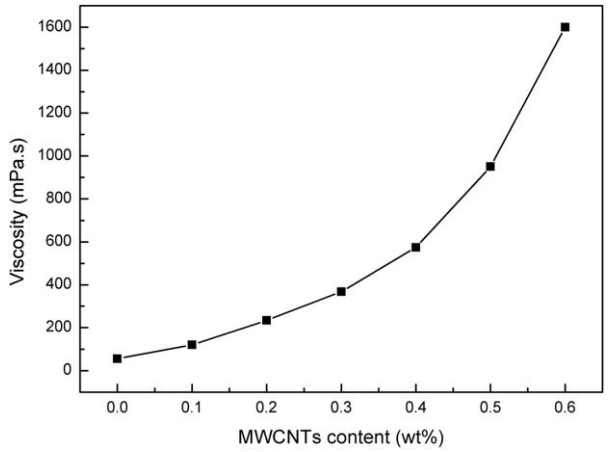

Figure 2. Viscosity values of the cyanate ester/epoxy resins with various mass contents of MWCNTs at 45°C.

immersion of the specimens and the clamps into liquid nitrogen. The specimen was prepared with outer dimensions of 4 × 8 × 24 mm^3, and the span was 16 mm.

Scanning Electron Microscopy (SEM). The morphology of the fracture surfaces after SBS tests were taken with a Hitachi-4300 SEM instrument. The fracture surface was coated with gold before SEM investigation to improve the conductivity.

Measurements of the Thermal Conductivity and Electrical Conductivity. The thermal conductivity was measured by homemade equipment[15] with a steady-state method over the temperature range from 77 to 300 K and calculated with the following equation:

$$\lambda = Q\frac{L}{\Delta T \times S} \tag{1}$$

where Q is the power supplied, L is the distance of the specimen, S is the cross section of the specimen, ΔT is the measured temperature difference, and λ is the thermal conductivity. The schematic of the homemade equipment is shown in Figure 1.

The alternating current conductivity of the composites was measured with a Precision Impedance Analyzer (Agilent 4294A) at temperatures from 175 to 300 K operated at 1 V over a frequency range from 10 to 106 Hz. The thickness of the specimen was 0.5 mm, and the diameter was 30 mm.

RESULTS AND DISCUSSION

Processing Characteristics

The VPI used in this experiment required low-viscosity mixtures to ensure efficient impregnation. The viscosity values of the suspensions with MWCNTs dispersed in cyanate ester/epoxy resins at 45°C are shown in Figure 2. We observed that the addition of low-content MWCNTs resulted in a significant increase in the viscosity. With the increase of the MWCNT content, the viscosity of the mixture increased rapidly. The viscosity of the mixture was as high as 1600 mPa s when the MWCNT content reached 0.6 wt %. The high viscosity of the mixture was bad for resin impregnation in woven glass fibers with VPI because of the nonuniform distribution of resins in the GFRP composite.[16] Therefore, the content of the MWCNTs was limited to 0.5 wt %.

The contents of the void were determined for GFRP composites with different levels of MWCNT contents. The void content of the composites was measured according to ASTM D 2734-09. The calculation of the volume percentage of the void (V_v) was as follows:

$$V_v = 1 - \left(\frac{W_f}{\rho_f} + \frac{W_r}{\rho_r}\right)\rho_c \tag{2}$$

where W_f and W_r are the weight percentages of the glass fibers and MWCNT/resin, respectively; ρ_f, ρ_r, and ρ_c are the densities of the glass fibers, MWCNT/resin, and GFRP composites, respectively. After calculation, the void content was estimated to be lower than 0.5 vol %.

ILSS

Figure 3 shows the deformation curves obtained from the SBS test at 300 and 77 K. We observed that all of the curves rose gradually during the early stage of loading and then dropped suddenly; this demonstrated a distinct failure because of the interlaminar shear failure. Moreover, the slope of the deflection curve increased with the increasing amount of MWCNTs; this illustrated that the composites became stiffer with the addition of the MWCNTs. Compared with the deflection curves at

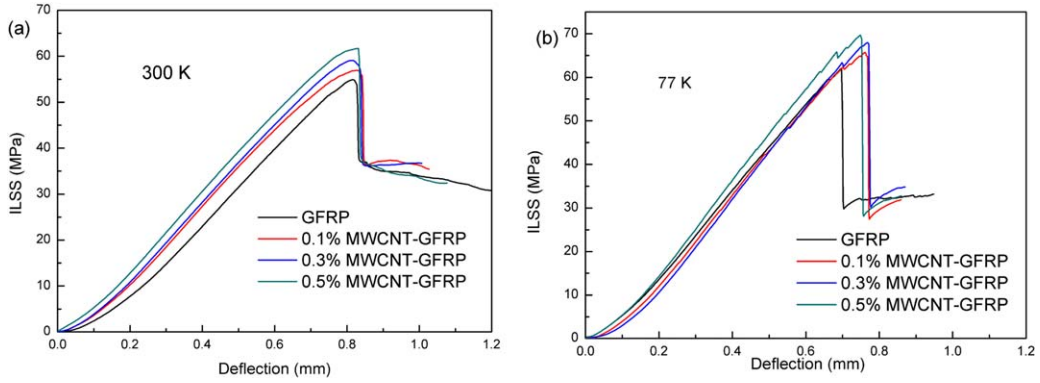

Figure 3. SBS test curves of the MWCNT-reinforced GFRP and GFRP at (a) 300 and (b) 77 K. [Color figure can be viewed in the online issue, which is available at wileyonlinelibrary.com.]

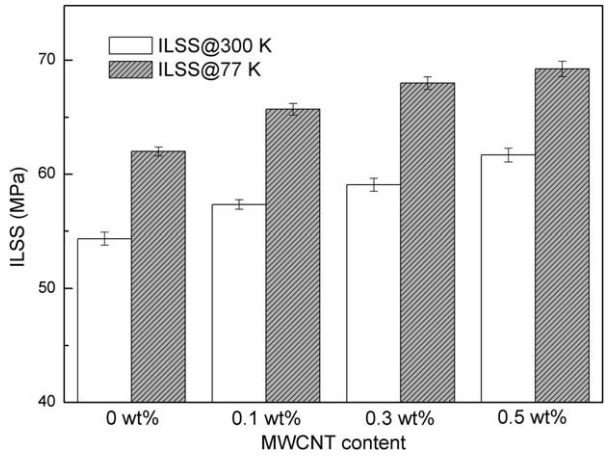

Figure 4. ILSS of the MWCNT-reinforced GFRP and GFRP at 300 and 77 K.

300 K, the curves at 77 K demonstrated a larger slope. A similar trend was observed for G-10CR woven laminates.[17]

The ILSS values of the GFRP and MWCNT–GFRP specimens at 300 and 77 K are shown in Figure 4. As the MWCNT mass content increased, the ILSS of the composites showed an increasing trend at both 300 and 77 K. With the addition of 0.5 wt % MWCNTs, the ILSS of the composites increased by 13.5 and 11.7% at 300 and 77 K, respectively. On one hand, the reinforcement mechanism was supported by SEM images. As shown in Figure 5(a,b), the matrix completely detached from the glass fiber because of weak interfacial bonding as the surface of the glass fiber was smooth with no matrix attached, and the fracture surface of the matrix was brittle. In comparison, for the MWCNT–GFRP composites [Figure 5(c,d)], the glass fibers were covered by a layer of matrix, and the fracture surface of the matrix was ductile. That is, the interfacial bonding between the matrix and glass fiber was improved with the addition of MWCNTs. On the other hand, the strength of the cyanate ester/epoxy matrix was enhanced by MWCNTs; this was attributed to the bridging/pulling-out mechanism.[18] Therefore, these two factors contributed to the enhancement of the ILSS.

Moreover, we found that the ILSS at 77 K showed great improvement compared with that at 300 K. This was because the strength and modulus of the cyanate ester/epoxy matrix were improved when the temperature decreased to 77 K. Because of the different coefficient of thermal expansion between the glass fibers and the matrix, the glass fibers were tightly clamped by the matrix, and thus, the interfacial bonding between the glass fibers and the matrix was improved. Therefore, the specimens at 77 K required a larger load to damage them. The fracture surfaces of the specimens at 300 and 77 K are shown in Figure 5(e,f), respectively. The fracture surface of the specimen at 77 K exhibited an increasingly hackly pattern compared with that at 300 K; this indicated that more surface energy was required to destroy the specimen at 77 K.

Thermal Properties

In the GFRP composites, the primary form of heat conduction was phonon transport because free movement of the electrons was not possible. The MWCNTs demonstrated ballistic transport properties, and phonon diffusion through the thermal transmission of the composites increased with addition of MWCNTs.[19] Therefore, the addition of MWCNTs may improve the thermal conductivity of composites. Figure 6 shows the thermal conductivities as a function of the temperature for the GFRPs with different levels of MWCNT mass contents. The thermal conductivity of the composites linearly increased when the temperature increased from 77 to 300 K; this was consistent with Garrett' research.[20] For the 0.5 wt % MWCNT–GFRP composites, the thermal conductivities were improved by 25.7 and 13.8% at temperatures of 300 and 77 K, respectively.

With simplifying hypotheses, it is possible to predict the thermal conductivity of the composites at 300 and 77 K with the Lewis–Nielsen equation, which is used to calculate the thermal conductivity of the two-phase systems.[21,22] On one hand, the cyanate ester/epoxy resin, together with glass-fiber woven, could be assumed to be one continuous phase. On the other hand, the MWCNTs dispersed into the GFRP composite resulted in another phase with improved thermal conductivity. The Lewis–Nielsen equation is given as follows:

$$\lambda = \lambda_m \left(\frac{1 + AB\varphi}{1 - B\varphi\psi} \right) \tag{3}$$

$$B = \frac{\lambda_f / \lambda_m - 1}{\lambda_f / \lambda_m + A} \tag{4}$$

$$\psi = 1 + \left(\frac{1 - \varphi_m}{\varphi_m^2} \right) \varphi \tag{5}$$

where λ_m is the thermal conductivity of the matrix, which was obtained in an experiment at both 300 and 77 K, and λ_f is the thermal conductivity of the CNTs, which was about 2000 W m^{-1} K^{-1} for 300 K and about 1000 W m^{-1} K^{-1} for 77 K.[23] ϕ_m is the maximum packing fraction of dispersed fillers, which was 0.52 for three-dimensional random packing. The constant A depends on the geometry and the orientation of the fillers in the composite and is related to Einstein's coefficient, particularly the aspect ratio, $2L/D$.[22] (L is the length of MWCNT and D is the outer diameter of MWCNT) ϕ is the volume fraction of fillers, which could be obtained on the basis of the density of the MWCNTs and the matrix. The density of the MWCNTs (ρ_{CNT}) was calculated by the following equation:

$$\rho_{CNT} = \frac{\rho_g (d_0^2 - d_i^2)}{{d_0}^2} \tag{6}$$

where d_0 and d_i are the outside and inside diameters of the MWCNTs, respectively, and ρ_g represents the density of the fully dense graphite structure.

The comparison of the experimental results and theoretical predictions of the thermal conductivity for the MWCNT composites is shown in Figure 7. The measured thermal conductivity was lower than the values predicted by the Lewis–Nielsen model. The possible reasons for the difference are given as following:

1. The Lewis–Nielsen model applies to large particles or fibers and overlooks the size effect of fillers when they show high aspect ratios.

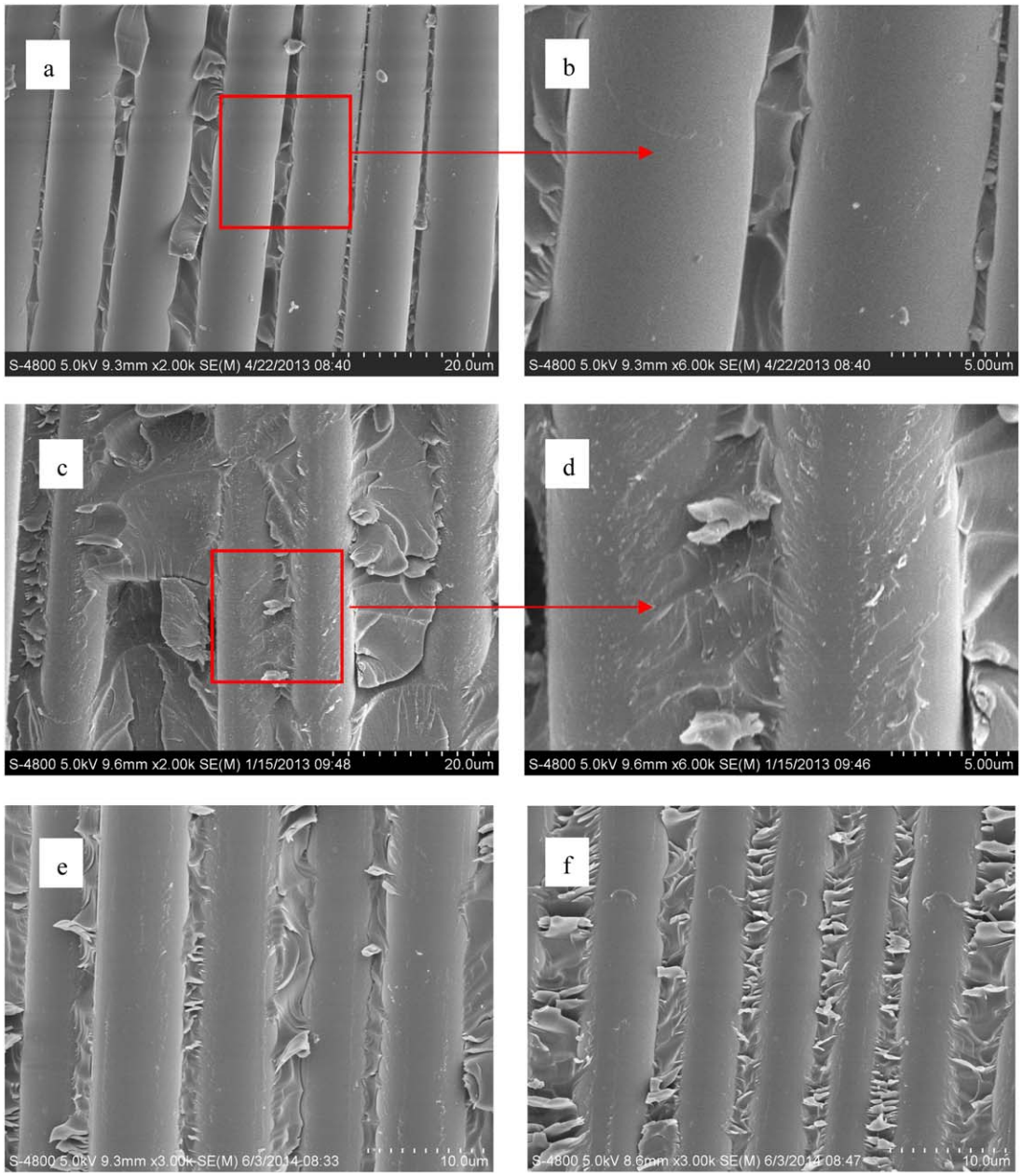

Figure 5. Fracture surface of the GFRP and 0.3 wt % MWCNT–GFRP: (a,b) GFRP at 300 K, (c,d) MWCNT–GFRP at 300 K, (e) GFRP with a low magnification at 300 K, and (f) GFRP with a low magnification at 77 K. [Color figure can be viewed in the online issue, which is available at wileyonlinelibrary.com.]

2. The Lewis–Nielsen model ignores the anisotropy of fillers.
3. The MWCNTs were assumed to be uniformly dispersed in the pure GFRP. However, because of the filtering effect,[18] the MWCNTs were not located between the fibers but in resin-rich areas; this resulted in different local concentrations.
4. The ultrathin PAA film on the MWCNT surface could impede thermal transmission in the composite.

Moreover, the deviation between the experimental results and the theoretical predictions at 77 K was more significant than that at 300 K. That was because the dominant phonon wavelength increased with decreasing temperature; thus, boundary phonon scattering was more significant at low temperature.[20] Because of the high aspect ratio of the MWCNTs, the phonon scatter occurring at the interface between the MWCNTs and the matrix became stronger at 77 K. Therefore, the experimental results of the thermal conductivity at 77 K were far below the theoretical predictions.

Electrical Conductivity

Figure 8 shows the dependence of the electrical conductivity of the composites with different MWCNT contents on the temperature, which ranged from 175 to 300 K, at a frequency of 10 kHz. We observed that at the same frequency, the electrical conductivity increased with increasing MWCNT content. The

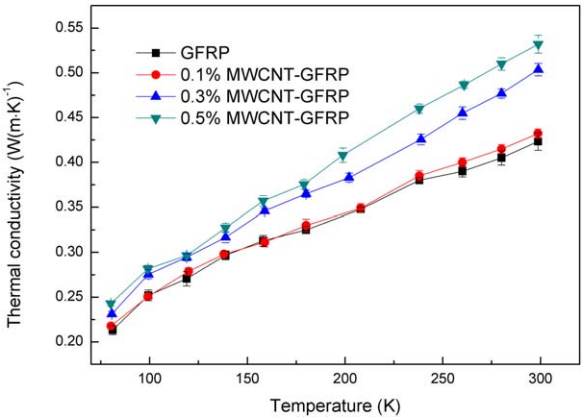

Figure 6. Thermal conductivities as a function of the temperature for the GFRPs with different MWCNT contents. [Color figure can be viewed in the online issue, which is available at wileyonlinelibrary.com.]

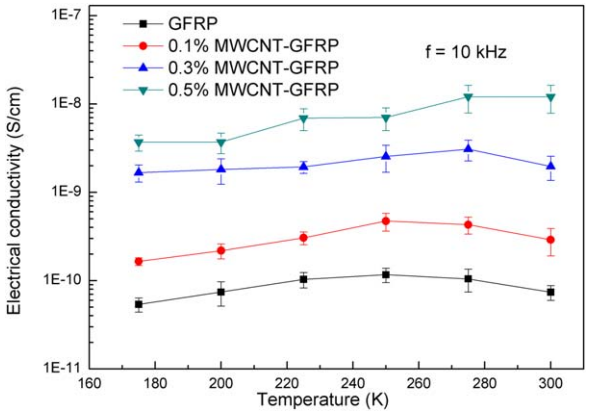

Figure 8. Volume resistivity and electrical conductivity as a function of the temperature for the GFRPs with different MWCNT mass contents. (f is the frequency in measuration). [Color figure can be viewed in the online issue, which is available at wileyonlinelibrary.com.]

electrical conductivity of the GFRP composites increased with the temperature until reached the maximum and then decreased, except for the GFRP with 0.5 wt % MWCNTs. The GFRP with 0.5 wt % MWCNTs showed an increasing trend, and perhaps the maximum value would appear after 300 K. The appearance of the peak value was attributed to the secondary relaxations in the polymer, which were associated with the molecular segment motion of the polymer.[24,25] Furthermore, the temperature corresponding to maximum value increased with the MWCNT content. The carboxyl groups on the surface of the MWCNTs provided the covalent bonds between the polymer matrix and the MWCNTs, and thus, the MWCNTs limited the mobility of the molecular chains. Therefore, the temperature of secondary relaxations of the polymer improved with increasing MWCNT content. Hence, the temperature corresponding to the maximum value increased.

The sudden insulator-to-conductor transition took place when the filler content reached the percolation threshold. Before the percolation threshold, the electrical conductivity linearly increased with increasing frequency and demonstrated the dielectric behavior of the insulator. Above the percolation threshold, the conductivity in the low-frequency region was not dependent on the frequency and demonstrated conductive behavior; this caused the material to convert from an insulator to a conductor.[26] Figure 9 shows the frequency-dependent alternating-current conductivities of the composites with various MWCNT contents at both 175 and 300 K. The alternating-current conductivity increased almost linearly as the frequency increased from 10 to 10^6 Hz; this indicated that the composites exhibited typical dielectric behavior at both 175 and 300 K. With the addition of 0.5 wt % MWCNTs, the GFRP composites achieved an electrical conductivity of 10^{-7} S/cm; this was above the electrical conductivity required for insulating materials to prevent electrostatic charging (10^{-8} S/cm).[6] That is, the composite with 0.5 wt % MWCNTs met the electrical requirements for static electrical dissipation. Conventional MWCNT-modified polymer composites usually have a low percolation threshold compared with traditional powder fillers because of the unique properties of the MWCNTs, including their high aspect ratio, inherently high conductivity, and high specific surface area. Guadagno et al.[27] investigated the effect of MWCNTs on the electrical behavior of the epoxy resin, and they found the percolation threshold to be lower than 0.1 wt %. Gojny et al.[10] dispersed functionalized DWCNTs into GFRP composites, and the percolation threshold was 0.3 wt %. This was larger than with

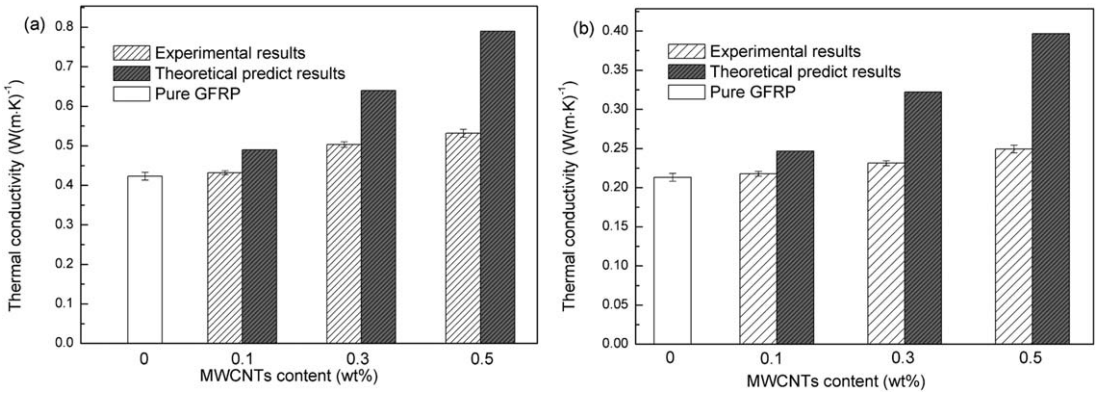

Figure 7. Comparison of the experimental results and theoretical predictions of the thermal conductivity for the MWCNT nanocomposites at (a) 300 and (b) 77 K.

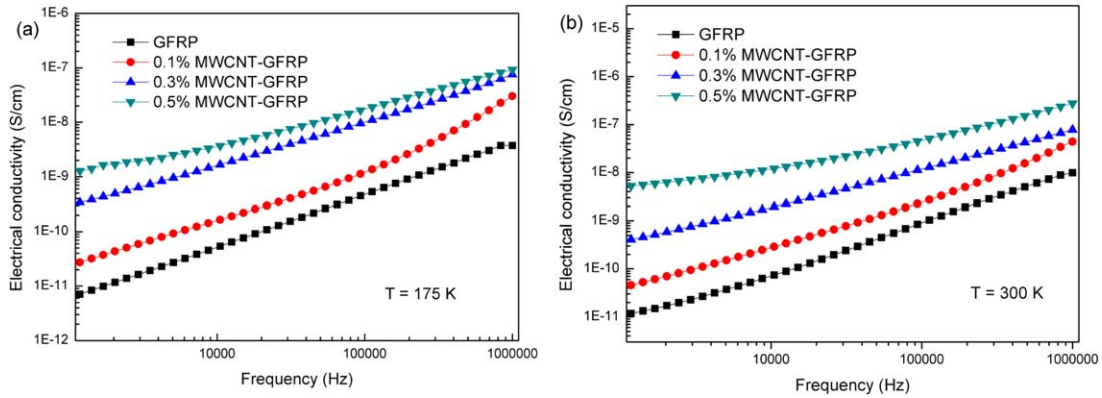

Figure 9. Effect of the frequency on the electrical conductivity of the GFRPs with different MWCNT contents at (a) 175 and (b) 300 K (b). *T* is the measuring temperature. [Color figure can be viewed in the online issue, which is available at wileyonlinelibrary.com.]

the as-received DWCNTs. Low percolation limited the content of MWCNTs used in the polymer matrix for an insulating material; thus, the mechanical and thermal properties showed little improvement because of the limited content. In our research, the composites retained nonconductive behavior with the addition of 0.5 wt % MWCNTs. The possible reasons are as follows:

1. Although the homogeneous dispersion of the functionalized MWCNTs in the matrix made it easy to form conductive paths, the conductivity path formed by the MWCNTs in the cyanate ester/epoxy matrix could be interrupted by the glass fibers.[10]
2. The tunneling currents could decrease relatively because of the ultrathin PAA film on the surface of the MWCNTs; thus, the conductivity increased slightly with increasing MWCNT content.[28,29]

Therefore, the addition of the MWCNTs into the glass-fiber-reinforced composites effectively improved the electrical conductivity and met the requirements for static electrical dissipation without changing the nonconductive behavior for insulating materials.

CONCLUSIONS

The effects of plasma-functionalized MWCNTs on the mechanical, thermal, and electrical properties of the GFRP composites were investigated at RT and cryogenic temperature. Improved ILSS and thermal conductivity at both RT and cryogenic temperature were observed with addition of MWCNTs at low contents. We also found that the electrical conductivity was improved significantly, but the composites still retained the nonconductive behavior. In particular, the composites with 0.5 wt % MWCNTs met the requirement for static electrical dissipation as an insulating material and demonstrated improved mechanical and thermal properties at all temperatures. The findings of this study suggest that plasma-functionalized MWCNTs could provide opportunities to modify the mechanical, thermal, and electrical properties of glass-fiber-reinforced composites at both RT and cryogenic temperature. These MWCNT composites, which had improved mechanical, thermal, and electrical properties, could be applied as novel insulating materials for both RT and cryogenic applications.

ACKNOWLEDGMENTS

This work was supported by the National Magnetic Confinement Fusion Science Program (contract grant number 2011GB112003), the National Natural Science Foundation of China (contract grant number 51377156), and the Key Laboratory of Cryogenics, Technical Institute of Physics and Chemistry, Chinese Academy of Sciences (contract grant number CRYOQN201303).

REFERENCES

1. Zhu, J.; Imam, A.; Crane, R.; Lozano, K.; Khabashesku, V. N.; Barrera, E. V. *Compos. Sci. Technol.* **2007**, *67*, 1509.
2. Chandrasekaran, V.; Advani, S.; Santare, M. *Carbon* **2010**, *48*, 3692.
3. Prokopec, R.; Humer, K.; Maix, R.; Fillunger, H.; Weber, H. *Fusion Eng. Des.* **2007**, *82*, 1508.
4. Karad, S. K.; Attwood, D.; Jones, F. R. *Compos. A* **2002**, *33*, 1665.
5. Prokopec, R.; Humer, K.; Maix, R. K.; Fillunger, H.; Weber, H. W. *Fusion Eng. Des.* **2009**, *84*, 1544.
6. Sandler, J.; Shaffer, M.; Prasse, T.; Bauhofer, W.; Schulte, K.; Windle, A. *Polymer* **1999**, *40*, 5967.
7. Humer, K.; Bittner-Rohrhofer, K.; Fillunger, H.; Maix, R.; Prokopec, R.; Weber, H. *Fusion Eng. Des.* **2006**, *81*, 2433.
8. Lin, L.-Y.; Lee, J.-H.; Hong, C.-E.; Yoo, G.-H.; Advani, S. G. *Compos. Sci. Technol.* **2006**, *66*, 2116.
9. Wooster, T. J.; Abrol, S.; Hey, J. M.; MacFarlane, D. R. *Compos. A* **2004**, *35*, 75.
10. Gojny, F. H.; Wichmann, M. H.; Fiedler, B.; Bauhofer, W.; Schulte, K. *Compos. A* **2005**, *36*, 1525.
11. Shen, Z.; Bateman, S.; Wu, D. Y.; McMahon, P.; Dell'Olio, M.; Gotama, J. *Compos. Sci. Technol.* **2009**, *69*, 239.
12. Shi, D.; Lian, J.; He, P.; Wang, L.; Van Ooij, W. J.; Schulz, M.; Liu, Y.; Mast, D. B. *Appl. Phys. Lett.* **2002**, *81*, 5216.
13. Li, J.; Wu, Z.; Huang, C.; Chen, Z.; Huang, R.; Li, L. *Colloids Surf. A* **2013**, *433*, 173.

14. Li, J.; Wu, Z.; Huang, C.; Liu, H.; Li, R. H. *Compos. Sci. Technol.* **2014**, *90*, 166.
15. Liu, H.; Xu, D.; Xu, P.; Huang, R.; Xu, X.; Li, L.; Gong, L. *J. Phys. Conf. Ser.* **2012**, *1434*, 1363.
16. Wu, Z.; Li, J.; Huang, C.; Huang, R.; Li, L. *Fusion Eng. Des.* **2013**, *88*, 3078.
17. Shindo, Y.; Wang, R.; Horiguchi, K. *J. Eng. Mater. Technol.* **2001**, *123*, 112.
18. Fan, Z.; Santare, M. H.; Advani, S. G. *Compos. A* **2008**, *39*, 540.
19. Han, Z.; Fina, A. *Prog. Polym. Sci.* **2011**, *36*, 914.
20. Garrett, K.; Rosenberg, H. *J. Phys. D* **1974**, *7*, 1247.
21. Pal, R. *Compos. A* **2008**, *39*, 718.
22. Nielsen, L. E. *Ind. Eng. Chem. Fundam.* **1974**, *13*, 17.
23. Osman, M. A.; Srivastava, D. *Nanotechnology* **2001**, *12*, 21.
24. Migahed, M.; Ishra, M.; Fahmy, T.; Barakat, A. *J. Phys. Chem. Solids* **2004**, *65*, 1121.
25. Montazeri, A.; Montazeri, N. *Mater. Des.* **2011**, *32*, 2301.
26. Han, C.; Gu, A.; Liang, G.; Yuan, L. *Compos. A* **2010**, *41*, 1321.
27. Guadagno, L.; De Vivo, B.; Di Bartolomeo, A.; Lamberti, P.; Sorrentino, A.; Tucci, V.; Vertuccio, L.; Vittoria, V. *Carbon* **2011**, *49*, 1919.
28. Wang, L.; Dang, Z.-M. *Appl. Phys. Lett.* **2005**, *87*, 042903.
29. Dang, Z. M.; Wang, L.; Yin, Y.; Zhang, Q. *Adv. Mater.* **2007**, *19*, 852.